Microbial Enhanced Oil Recovery: Modelling and Simulations

Théophile Mbuyi Tshibangu (theo@aims.ac.za)
African Institute for Mathematical Sciences (AIMS)

Supervised by: Dr Antoine Tambue
African Institute for Mathematical Sciences and University of Cape Town (UCT), South Africa

18 May 2017

Submitted in partial fulfillment of a structured masters degree at AIMS South Africa

Abstract

Energy is one of the most essential needs of modern day human beings. One of the largest source of the energy consumed around the world is crude oil. Unfortunately, this form of energy is not renewable and the world reserves have significantly decreased the last century. Scientists are therefore looking for new techniques of enhanced oil recovery which must be environmentally friendly and inexpensive.

Microbial Enhanced Oil Recovery (MEOR) is investigated in this work. In this technique, two species are injected in the subsurface reservoir: microbes and nutrients. Microbes, especially bacteria, consume nutrients and produce metabolites and other microbes. These products contribute to the change of oil and water properties. For metabolites, there are two types which are very important: surfactant and polymer. The growth rate of bacteria and metabolite is done using Michaelis-Menten and Monod models. However, the positive effect of surfactant consists in reducing the interfacial tension between water-oil interface. This increases the relative permeability of oil and the model used is Corey interpolation. Though many works have neglected the effect of polymers, in this work we have considered three best models based on the change of dynamic viscosity and an approach of the influence of the polymer in formation of biofilm with both bacteria. Thus, the realistic MEOR model found is a system of six partial differential equations from mass balance. The discretization of these PDEs is done using finite volume method.

Unfortunately, the global model found needs more time for implementation and more knowledge in programming. At this instance, we have just implemented in Python a simple model under some assumptions. Overall, the result has shown that MEOR model with only surfactant could produce up to 85% of Oil Initially In Place (OIIP) while water flooding adds about 10% of OIIP to primary process.

Declaration

I, the undersigned, hereby declare that the work contained in this research project is my original work, and that any work done by others or by myself previously has been acknowledged and referenced accordingly.

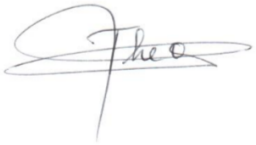

Théophile Tshibangu Mbuyi, 18 May 2017

Contents

1. Introduction

Nowadays, although science has discovered renewable energy technologies, more than 85% of energy used in the world for human needs comes from reserve fossils and the majority thereof comes from crude oil (Huppert and Neufeld, 2014). Oil does not just serve as an energy resource, it is also used in petrochemical production (production of plastic for example) where other kinds of energy resources cannot challenge crude oil. With the steady increase in world's population, we see a decline in oil reserves.

Recently, many researchers are looking for others techniques of enhancing oil recovery because, traditional methods of enhanced oil recovery (EOR) leave more residual oil trapped in capillary pores or in unswept areas into the subsurface reservoirs. Microbial enhanced oil recovery (MEOR) is a chemical method and was discovered in the 1920s (Lazar et al., 2007). The idea of using microbes in oil recovery started with Beckman Back in 1926 and was performed by Zobell in 1946 (Eldeen et al., 2013). In MEOR, bacteria and nutrients are injected in water into a subsurface reservoir. There, bacteria consume nutrients and produce metabolites. These metabolites possess the qualities that modify oil, saline water and rock properties. The first idea in using MEOR process is to make water heavy and henceforth water will move slowly allowing oil to move quickly. This is done by both surfactant and polymer. Metabolites polymer increase the viscosity of water while metabolites surfactant reduce the interfacial tension (IFT). Secondly, the biofilm produced by bacteria and polymer living in saline water contributes to clog the thief zones (zones of high permeability susceptible of to have the leakage of substance and pressure) and therefore increases the pressure in the subsurface (Amundsen, 2015). MEOR technologies are becoming accepted worldwide as effective and environmentally friendly approaches to improving oil production. They use low energy, are inexpensive and their processes need minor modifications. They are more easily applied than other EOR methods and are particularly suited for carbonate oil reservoirs where some EOR technologies cannot be applied with good efficiency (Lazar et al., 2007). To model MEOR methods, the mass balance equations for fluid flow underground and transport equation must be evoked. However,for microbial modelling, many previous works have considered two phases flow oil-water (Nielsen et al., 2010a; Amundsen, 2015), but only (Islam, 1990) has presented three phases flow oil-water-gas. Also, many works have shown that the most important metabolites in microbial recovery process are polymer or surfactant and gas. However, those who have modelled polymer neglect to take into account the new velocity of polymer. Amundsen (2015), in neglecting this, have assumed that the adsorbed polymer (polymer in biofilm) concentration is too small, while by the definition of biofilm, polymer is one of the most constituent. Those assumptions carry out could give erroneous descriptions and invalid the results.

The aim of this project is to make a more realistic model of Microbial effect in enhancing oil recovery in considering the new velocity of polymer and its contribution in the constitution of biofilm.The mathematical model will be discretized using Finite Volume Methods and simulations are performed in Python. For that, except the introduction and the conclusion, the project will have 3 chapters. The first chapter will be focused on the basic two phase flow model in a porous medium and a general case of transport model. The second will model the growth rate of bacteria and metabolites, choose a model for the polymer, surfactant and biofilm effect and give the assumptions for the full model. As we expect to get a system of partial differential equations, the third chapter will solve the problem by using the discretization in time and in space. But to show the effect of MEOR, the implementation will be done in Python on a simplified model (using some assumptions on the full model) because the implementation of the full model will require more time and work.

2. Oil Recovery and Model Flow in Porous Media

This chapter will briefly explain the process of oil recovery and will focus on a microbial process and its advantages. In addition, we will give an understanding of multi-phase flows in a porous medium and will give a full model of two phase flows (oil and water). The transport equation for a general case will also be given.

2.1 Oil Recovery Processes

Oil recovery is a set of processes by which crude oil is extracted from the beneath Earth's surface. The process starts by drilling well into a subsurface reservoir containing natural oil. The conventional oil recovery processes are done in three stages. In primary recovery, after the drilling of wells, natural mechanisms contribute to pushing oil to surface. The process starts with natural underground saline water pushing oil downward. After that, natural gas and gas contained in oil expand upward and by gravity oil flows to the well of production. This recovery process is therefore caused only by natural driving forces. When these natural driving forces are failing, there are some mechanical techniques set at the well of production used to pull oil up. Usually the primary recovery process yields about 5-15% of Oil Initially In Place (OIIP) (Wikipedia, a). In secondary recovery, as natural pressure in the reservoir fails to bring oil at the recovery wellbore, injections of external fluids increase underground pressure and give an artificial reservoir drive. The fluids usually used are offshore saline water, natural gas or lift gas. This process adds 15-20% of the OIIP to the primary recovery (Eldeen et al., 2013). Primary and secondary oil recovery techniques give 35-40% of the OIIP depending on the nature of the oil and the rock (Lacerda et al., 2012). This recovery factor is very small and it leaves a considerable amount of useful oil in the subsurface. It is for this reason that the third process called Enhanced Oil Recovery (EOR) is used.

2.1.1 Enhanced Oil Recovery (EOR). Tertiary recovery is called traditional enhanced oil recovery. There are three different processes: the thermal enhanced oil recovery (TEOR), the chemical flooding process and the miscible flooding. First of all, the thermal method decreases the viscosity of oil. This method is particularly useful for heavy oil. The process consists of injecting the hot water or the steam flooding in the subsurface reservoir. By conduction, the heat is transferred into the oil and will modify its dynamic viscosity. Henceforth, oil will move quickly to the well of production. Secondly, the chemical flooding method consists of injecting the external surfactant and/or polymer into the subsurface reservoir where the chemical substances will alter properties of oil and water. Finally, the miscible flooding method uses the carbon dioxide or the di-nitrogen or flue gas that modify the physical conditions in the reservoir. Usually these EOR processes add about 5-15% of OIIP to the previous processes (Wikipedia, a). This shows that, depending on the nature of the oil and the rock, the tertiary processes could be inefficient.

In addition to these methods of enhancing oil recovery, microbial and electromagnetic methods are advanced technologies used nowadays to recover residual oil efficiently. This work will only present the microbial technique as it is the most inexpensive method.

2.1.2 Microbial Enhanced Oil Recovery. The principle is that microbes consume nutrients and produce the micro-organisms by a metabolism process. These micro-organisms are called metabolites and are beneficial in enhancing oil recovery. There are many kind of metabolites produced depending on the

nature of the microbes and nutrients species. In terms of their role (Romero-Zerón, 2012; Yen, 1989; Amundsen, 2015), polymer and surfactant metabolites are the most important in the microbial process of oil recovery. Table 2.1 shows the effect of six kind of metabolites.

Metabolites	Effects
Acid	-Improves the permeability and the porosity by degradation of the rock -Reduction of oil viscosity by production of the CO_2 when reacting with carbonates
Solvents	-Dissolving the oil
Biomass	-Selective/non-selective plugging -Altering the wettability -Reduction of oil viscosity
Gases	-Pressurization of the reservoir -Viscosity reduction
Surfactants	-Reduction of the IFT -Emulsification
Polymers	-Mobility control or increasing water dynamic viscosity -Selective/non-selective plugging

Table 2.1: Metabolites of MEOR and their effects (Romero-Zerón, 2012; Yen, 1989)

Polymers produced in the saline water increase the viscosity of water which causes a large displacement of oil. Surfactants, as a monomer hydrophilic and lypophilic (Skiftestad, 2015) reduce by this duality the interfacial tension (IFT) between oil and water. Hence, they contribute to the mobilizing of residual oil which would otherwise remain trapped in capillary zones.

Due to the difficult conditions in the subsurface reservoir (high temperature, natural gas) and difficulty to supply oxygen into the subsurface reservoir, the most used microbes are Bacillus and Clostridium (BC) which are aneoribic bacteria (Nielsen et al., 2010b). Figure 2.1 shows the process of microbial enhanced oil recovery from the injection of bacteria and nutrients passing through the reservoir to the production of crude oil.

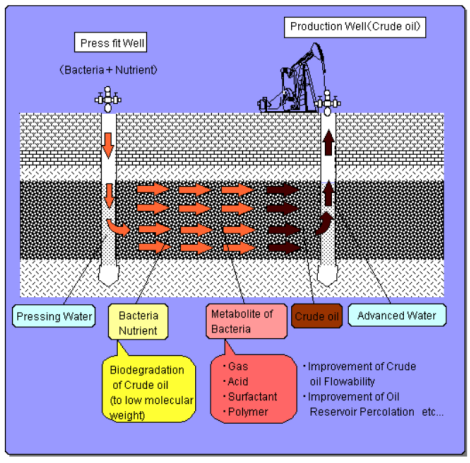

Figure 2.1: MEOR process in subsurface resevoir (Eldeen et al., 2013).

Both bacteria and polymer in saline water produce a biofilm which clogs thief zones (zones of high

permeability) of reservoir and hence change the permeability of the rock. This effect influences the pressure in the subsurface reservoir and causes the increase of oil mobility.

2.2 Model Flow in Porous Medium

In oil recovery process, there is water and oil flowing in a porous medium. A porous medium is a solid reservoir with pores or void spaces. These pores allow fluid to move continuously. Due to the size of pores, modelling fluid flow on a micro-scale is difficult. A better approach of Representative Elementary Volume (REV) is commonly used.

2.2.1 Representative Elementary Volume (REV). A REV contains a representative number of pores which fix the porosity and the permeability of the rock. Only the average of these microscopic physical parameters into REV will be considered in order to simplify the model.

The first propriety of the rock is the porosity ϕ. It is a ratio of the void volume V_0 over the total volume of REV V. The porosity

$$\phi = \frac{V_0}{V}\,, \tag{2.2.1}$$

is a dimensionless number that ranges between 0 and 1. A very porous medium has its porosity approaching 1, and a very compact medium approaches 0.

The second property of the rock is the absolute permeability $\mathbf{K}$. It is the ease with which fluid flows through the REV. Absolute permeability is expressed in Darcy unit $(1D = 0.986922um^2)$ (Lake, 1989). The Kozeny-Carman equation gives a relationship between these two characteristics of REV:

$$\mathbf{K} = \frac{1}{8\tau A_v^2}\frac{\phi^3}{(1-\phi)^2}\,, \tag{2.2.2}$$

where A_v is the total surface area of the rock over its total volume and τ, called turtuosity, is the pore length over the distance between pore entrance-exit. In general, flows in porous media are anisotropic and heterogeneous. Therefore the permeability is modelled as a tensor $\mathbf{k}$. In a multiple phase flow, the concept of relative permeability is more useful because it determines the parameters found experimentally (see Section 2.2.5).

2.2.2 Porous Medium Flow. A fluid indexed by i is described by its density ρ_i, its dynamic viscosity μ_i and its saturation S_i in a porous medium. The density describes the amount of mass fluid contained in a unit volume, while the dynamic viscosity expresses the resistance of flowing for a fluid. The saturation gives the ratio of a volume of fluid i over the total volume of fluid contained in REV:

$$S_i = \frac{\text{Volume of fluid } i \text{ in REV}}{\text{Total volume of fluid in REV}}\,, \tag{2.2.3}$$

such that $\sum_i S_i = 1$ with $i \in [1, n]$ and n the number of fluids in the REV.

Darcy's equation

Darcy's equation is an experimental equation governed by fluid flow in porous media (Huppert and Neufeld, 2014). Darcy's equation is derived from the Navier-Stokes equation for a quasi parallel steady flow with small Reynold's number. This approximation comes from small size of pores in which fluid is flowing. Darcy's equation (from Henry Darcy) gives the vector velocity of fluid:

$$\overrightarrow{u} = -\frac{1}{\mu}\mathbf{k}(\nabla p - \rho\overrightarrow{g})\,, \tag{2.2.4}$$

where $\overrightarrow{g}$ is a gravitational vector acceleration and p is the pressure.

Mass conservation equation

Let Ω be a domain (volume control), $\overrightarrow{n}$ the outward normal vector to the boundary $\delta\Omega$. If any substance flow with velocity $\overrightarrow{u}$ through the volume in time interval t and $t+\delta t$, and if we call $\mathbf{q}$ the source term (representing the flux of the substance injected or produced in the same time interval), then the mass conservation equation (Landau and Lifchitz, 1971) is

$$\frac{\partial}{\partial t}\int_{\Omega}\phi\rho dV + \int_{\delta\Omega}\rho\overrightarrow{u}.\overrightarrow{n}dA = \int_{\Omega}\mathbf{q}dV\,. \tag{2.2.5}$$

Using the Divergence Theorem, this equation leads to :

$$\int_{\Omega}\left(\frac{\partial}{\partial t}(\phi\rho) + \nabla.(\rho\overrightarrow{u})\right)dV = \int_{\Omega}\mathbf{q}dV\,. \tag{2.2.6}$$

The Equation (2.2.6) is satisfied for the domain Ω, which is chosen arbitrarily. Finally, the mass conservation is expressed by:

$$\frac{\partial}{\partial t}(\phi\rho) + \nabla.(\rho\overrightarrow{u}) = \mathbf{q}\,. \tag{2.2.7}$$

Equations (2.2.4) and (2.2.7) represent the mathematical models of a fluid flows in the porous medium. In this work, we need to model two phases flow (oil and water).

2.2.3 Multi-Phase flow. Let us use w and o as water and oil indices respectively. Since water and oil have different properties, we need to model them separately. For multiphase flow, the concept of saturation is evoked and leads to:

$$\begin{aligned}\overrightarrow{u}_i &= -\frac{1}{\mu_i}\mathbf{k}(\nabla p - \rho_i\overrightarrow{g})\,,\\ \frac{\partial}{\partial t}(\phi\rho_i S_i) + \nabla.(\rho_i\overrightarrow{u}_i) &= \mathbf{q}_i\ ,\end{aligned} \tag{2.2.8}$$

with $i\in\{o,w\}$ for oil and water.

In reality, in the subsurface reservoir, the volatility of oil could be increased due to the differences in surface and subsurface conditions (temperature, pressure) and therefore gases maybe produced. The properties of fluid will be affected separately. A volume factor β (Fanchi, 2005) is useful to model the compressibility of fluid in REV. This volume factor lies between 0 and 1. It approaches 1 for oil which is not affected by the change of conditions in the reservoir. The density in REV is

$$\rho = \frac{\rho_{sc}}{\beta}\,, \tag{2.2.9}$$

where ρ_{sc} is the density in surface condition.

From Equation (2.2.8), the mass balance equation becomes

$$\frac{\partial}{\partial t}\left(\frac{\phi S_i}{\beta_i}\right) + \nabla.\left(\frac{\overrightarrow{u}_i}{\beta_i}\right) = \widetilde{\mathbf{q}}_i\,, \tag{2.2.10}$$

where $\widetilde{\mathbf{q}}_i = \dfrac{\mathbf{q}_i}{\rho_{sc,i}}$.

2.2.4 Transport equation. Since, water will transport bacteria, nutrients and metabolites, it is very important to use the transport equation. Let c_j be the concentration of particles transported into fluid i, and c_{inj} the injected substance concentration. The transport equation in case of no diffusion is given by

$$\frac{\partial}{\partial t}\left(\frac{\phi S_i c_j}{\beta_i}\right) + \nabla.\left(\frac{\overrightarrow{u}_i c_j}{\beta_i}\right) = \widetilde{\mathbf{q}_{ij}}\,, \tag{2.2.11}$$

where $\widetilde{\mathbf{q}_{ij}} = \widetilde{\mathbf{q}}_i c_{inj}$ is the source term of the particles.

2.2.5 Relative Permeability. The real reservoir does not have the same pore size and also may contain a virtual impermeable layer in particular regions. Moreover, rocks are heterogeneous and fluid does not flow in them in the same direction with the same properties. For these reasons, the concept of relative permeability is therefore needed. Henceforth, for each fluid i, its relative permeability $\mathbf{k}_{r,i}$ is a better expression of permeability. For each fluid, the total effective permeability is obtained as a product of relative and absolute permeability:

$$\mathbf{k}_{ef,i} = \mathbf{k}_{r,i}(S_i, c)\mathbf{k}\,. \tag{2.2.12}$$

In the last equation, the relative permeability depends on saturation and concentration of substances inside of the fluid (Nielsen et al., 2010b). Unfortunately, because of the complexity of fluid flow in the subsurface, relative permeability curves are not available. Until now, many works have used Corey equation (Banat et al., 2000; Nielsen et al., 2010a; Amundsen, 2015) as the best experimental model,

$$\begin{aligned}
\mathbf{k}_{r,w} &= \mathbf{k}_{r,wor}.\left(\frac{S_w - S_{wi}}{1 - S_{or} - S_{wi}}\right)^a,\\
\mathbf{k}_{r,o} &= \mathbf{k}_{r,owi}.\left(\frac{1 - S_w - S_{or}}{1 - S_{or} - S_{wi}}\right)^b,
\end{aligned} \tag{2.2.13}$$

where S_w is the water saturation, S_{wi} is the initial water saturation, S_{or} is the residual oil saturation, $\mathbf{k}_{r,wor}$ is the endpoint relative permeability for water at saturation $1 - S_{or}$ and $\mathbf{k}_{r,owi}$ is the endpoint relative permeability for water at saturation S_{wi}, a and b are Corey exponents respectively for water and oil. The residual term describes the oil phase trapped and immobilised in the pores.

Thus for two phases flow in a porous medium, the mass balance equations for oil and water are

$$\begin{aligned}
\frac{\partial}{\partial t}\left(\frac{\phi S_o}{\beta_o}\right) + \nabla.\left(\frac{\overrightarrow{u}_o}{\beta_o}\right) &= \widetilde{\mathbf{q}_o}\,,\\
\frac{\partial}{\partial t}\left(\frac{\phi S_w}{\beta_w}\right) + \nabla.\left(\frac{\overrightarrow{u}_w}{\beta_w}\right) &= \widetilde{\mathbf{q}_w}\,,
\end{aligned} \tag{2.2.14}$$

and the Darcy equations are

$$\begin{aligned}
\overrightarrow{u}_o &= -\frac{\mathbf{k}_{r,o}}{\mu_o}\mathbf{k}(\nabla p_o - \rho_o \overrightarrow{g})\,,\\
\overrightarrow{u}_w &= -\frac{\mathbf{k}_{r,w}}{\mu_w}\mathbf{k}(\nabla p_w - \rho_w \overrightarrow{g})\,.
\end{aligned} \tag{2.2.15}$$

At this instance, a full model must include the effect of capillary pressure between oil and water as two miscibles fluid.

2.2.6 Capillary Pressure and Interfacial Tension. Instead of having only gravitational and gradient pressure, there is another effect between two immiscible phase flow that cuts the curved fluid-fluid interface. This fact leads to the force called "capillary force" (Bastian, 1999). According to fluid dynamics, this effect is caused by the dynamic component of pressure. The capillary pressure through the interface surface between oil and water is

$$p_c = p_o - p_w \,, \tag{2.2.16}$$

and depends on the water saturation (Nordbotten and Celia, 2011). Capillary pressure therefore influences the surface tension or interfacial tension (IFT) between oil and water. Inside a pore, Young-Laplace Model proposes a relation between the IFT σ and the capillary pressure as

$$p_c = \frac{2\sigma cos\theta}{r_{eff}} \,, \tag{2.2.17}$$

where θ is the angle between solid and interface and r_{eff} is the effective curvature radius of the pore as shown in Figure 2.2.

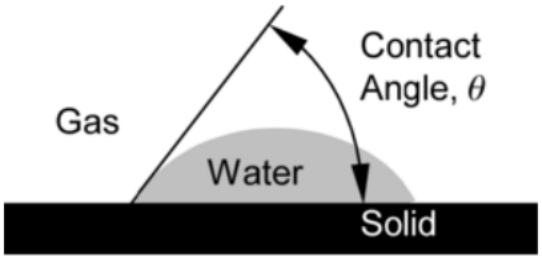

Figure 2.2: A droplet of water in gas on a solid (Lake, 1989).

Another concept must be considered if there is no equilibrium on the interface. In this case, the dynamic pressure will be added depending on the concentration c and saturation S. Equation (2.2.16) and (2.2.17) lead to (Hassanizadeh et al., 2002):

$$p_o - p_w = p_c(S, c) - \tau_c \frac{\partial S}{\partial t} \,, \tag{2.2.18}$$

where τ_c is a dynamic capillary. The total pressure p is the average of oil and water pressure

$$p = \frac{p_w + p_o}{2} \,. \tag{2.2.19}$$

To simplify the model, we consider that there is equilibrium in pressure on the interface. Therefore, the oil pressure and water pressure are given by:

$$\begin{aligned} p_o &= p + \frac{p_c}{2} = p + \frac{\sigma cos\theta}{r_{eff}} \,, \\ p_w &= p - \frac{p_c}{2} = p - \frac{\sigma cos\theta}{r_{eff}} \,. \end{aligned} \tag{2.2.20}$$

These expressions of pressure for oil and water found in Equation (2.2.20) must be substituted in Equation (2.2.15). Finally Darcy's law with Equation (2.2.14) give a full model of two phases flow in the subsurface porous medium. The next step is to model the contribution of reactions (Microbial effect) in enhancing oil recovery.

2.3 Summary

This chapter shown the advantages of using the microbial process to enhance oil recovery after the traditional processes. As oil and water flow in the subsurface reservoir, the model of two phases involves Darcy's law (see Equation(2.2.15)) and mass balance equations (see Equation(2.2.14)). The relative permeabilities (see Equation (2.2.13)) was given because the rock is considered anisotropic. The realistic model needs to include the capillary pressure concept (see Equation(2.2.20)). However, the transport equation for any j particle into fluid i has also been mentioned (see Equation(2.2.11)) for the general case by neglecting the diffusion term.

3. Microbial Enhanced Oil Recovery Modelling

In the last model of fluid flow in a porous medium, microbes especially bacteria, nutrients, metabolites and biofilm models must be added to form a complete microbial model. In saline water, after consuming nutrients, bacteria produce metabolites and reproduce other bacteria. Surfactants and polymers are the important kinds of metabolites in enhancing oil recovery. In this chapter, we model them and add the model of the biofilm. We aim to model the contribution of adsorbed polymers in the model, which has been neglected in previous work. We will use for these models, some experimental relations.

3.1 Bacteria Modelling

The choice of anaerobic bacteria as microbes for the microbial method depends on the rate of growth, type of nutrients consumed, kinds of metabolites produced and quality of biofilm produced by them. Michaelis-Menten kinetics model is used for modelling the growth rate of the products in the reaction (Lobry, 2008; Wikipedia, b). Let us call B the concentration of bacteria (substance and product) and N the concentration of nutrients (substrate). The growth rate η_b of the bacteria is

$$\eta_b = \eta_{b,max} \frac{N}{K_b + N}\,, \tag{3.1.1}$$

where K_b represents the substrate concentration at which the reaction rate is half of the maximum growth rate $\eta_{b,max}$. In addition, metabolites are also the product of reaction. A similar reasoning could be used for their growth rate. Let M be the concentration of metabolites, their growth rate is:

$$\eta_m = \eta_{m,max} \frac{(N - N_{crit})}{K_m + (N - N_{crit})}\,, \tag{3.1.2}$$

where N_{crit} is the critic nutrient concentration necessary for boosting the metabolite production and K_m represents the substrate concentration at which the reaction rate is half of the maximum growth rate $\eta_{m,max}$. Bacteria and metabolites are indexed by b and m respectively.

Using the Monod model (Nielsen et al., 2010a), the source term or the subsurface reaction is a product of specific growth rate η_i, bacteria concentration B and yield coefficient Y_i. The yield coefficient is used to describe the reproduction of bacteria by bacteria and production of metabolites by bacteria in the same time such that $\sum_{i=b,m} Y_i = 1$ (Nielsen et al., 2010a).

The reaction terms in subsurface reservoir are

$$R_b = \eta_b B Y_b\,, \tag{3.1.3}$$
$$R_m = \eta_m B Y_m\,. \tag{3.1.4}$$

Nutrients do not reproduce anything, but they are consumed, therefore their depletion leads to the reaction term

$$R_n = -R_b - R_m\,. \tag{3.1.5}$$

The source term $\mathbf{q}_i$ in conservation of mass is for injected substances while the reaction term R_j is for produced and depleted substances.

We make the assumption that every substance injected in water will flow with the same water velocity. The mass conservation for oil, water, bacteria, metabolites and nutrients are:

$$\frac{\partial}{\partial t}\left(\frac{\phi S_o}{\beta_o}\right) + \nabla.\left(\frac{\overrightarrow{u}_o}{\beta_o}\right) = \widetilde{\mathbf{q}_o}\,, \tag{3.1.6}$$

$$\frac{\partial}{\partial t}\left(\frac{\phi S_w}{\beta_w}\right) + \nabla.\left(\frac{\overrightarrow{u}_w}{\beta_w}\right) = \widetilde{\mathbf{q}_w}\,, \tag{3.1.7}$$

$$\frac{\partial}{\partial t}\left(\frac{\phi S_w B}{\beta_w}\right) + \nabla.\left(\frac{\overrightarrow{u}_w B}{\beta_w}\right) = \mathbf{q}_b + R_b\,, \tag{3.1.8}$$

$$\frac{\partial}{\partial t}\left(\frac{\phi S_w M}{\beta_w}\right) + \nabla.\left(\frac{\overrightarrow{u}_w M}{\beta_w}\right) = R_m\,, \tag{3.1.9}$$

$$\frac{\partial}{\partial t}\left(\frac{\phi S_w N}{\beta_w}\right) + \nabla.\left(\frac{\overrightarrow{u}_w N}{\beta_w}\right) = \mathbf{q}_n + R_n\,. \tag{3.1.10}$$

3.2 Metabolites Modelling

Only metabolites surfactants and metabolites polymer will be modelled. Their model will give the effective values of properties for both rock and fluids due to the microbial effect.

3.2.1 Surfactant. There is an effect between interface fluid-fluid immiscible creating a capillary trapping. The main role of the surfactant consists of reducing this IFT in three or four of its magnitude and therefore promote the mobility of oil. This role is done when surfactant molecules are seeking out the facial boundary between oil and water in the reservoir. The updated IFT σ^* is given by an empiric expression (Nielsen et al., 2010a)

$$\sigma^*(M_s) = \sigma\frac{1 + l_1 - \tanh(l_3 M_s - l_2)}{1 + l_1 - \tanh(-l_2)}\,, \tag{3.2.1}$$

as function of surfactant concentration M_s and previous IFT σ. The index * is related to the modified values, or the effective values, after the contribution or the positive effect of the substance and l_1, l_2, l_3 are constant for various surfactant properties.

Figure 3.1 shows the effect of surfactant in reducing capillary pressure for different values of parameters l_1, l_2, l_3. The change of IFT causes the change of the relative permeabily curves. The most common approaches used (Nielsen et al., 2010a) for modelling this are:

- The capillary number.
- The Coasts's interpolation.
- The Corey's interpolation.

1. **The Capillary number,** N_{ca}**,** is a dimensionless number which depends on the updated IFT, the characteristic of the linear velocity u_w and the water viscosity μ_w. It is given by

$$N_{ca} = \frac{\mu_w u_w}{\sigma^*}\,. \tag{3.2.2}$$

The capillary number is inserted in the model through the residual oil saturation. The modified oil saturation is given by

$$S^*_{or} = S_{or}\frac{1 + l_2 - \tanh(l_1(N^*_{ca}) - l_3)}{1 + l_2 - \tanh(l_1(N_{ca}) - l_3)}\,. \tag{3.2.3}$$

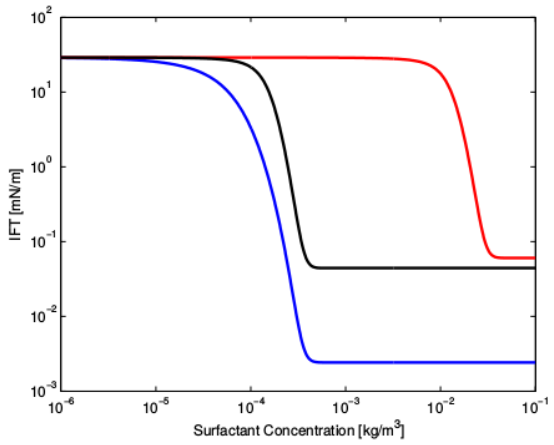

Figure 3.1: A graph of three different surfactant's effects on IFT. They show different curvatures from the minimum to the critical concentration values (Nielsen et al., 2010a).

2. **The Coats's interpolation between relative permeability curves** is used for modelling the change of relative permeabilities of the miscible fluids due to the change of the IFT. Let us define a function

$$f(\sigma^*) = \left(\frac{\sigma^*}{\sigma}\right)^{1/\epsilon}, \tag{3.2.4}$$

with ϵ an exponent ranging between 4 and 10 (Nielsen et al., 2010a). The new values of residual oil and initial water saturations are

$$S^*_{wi} = f(\sigma^*)S_{wi}\,, \tag{3.2.5}$$
$$S^*_{or} = f(\sigma^*)S_{or}\,. \tag{3.2.6}$$

Henceforth, the new expressions of the relative permeability curves depend on $f(\sigma^*)$ such that,

$$\begin{aligned} \mathbf{k}^*_{rw} &= f(\sigma^*)\mathbf{k}_{rw,base} + (1 - f(\sigma^*))\mathbf{k}_{rw,misc}\,, \\ \mathbf{k}^*_{ro} &= f(\sigma^*)\mathbf{k}_{ro,base} + (1 - f(\sigma^*))\mathbf{k}_{ro,misc}\,, \end{aligned} \tag{3.2.7}$$

where $\mathbf{k}_{ri,misc}$ is the straight line approaching the full miscibility of fluid i and $\mathbf{k}_{ri,base}$ is the relative permeability curve at large value of IFT.

3. **The interpolation of relative permeability parameters in Corey method** is similar to Coats's method where the interpolated parameters (modified Corey parameters a and b) modify the relative permeability curves and update them. The updated values in Corey's Equation (see Equation(2.2.13)) are found using:

$$S^*_{wi} = f(\sigma^*)S_{wi}\,, \tag{3.2.8}$$
$$S^*_{or} = f(\sigma^*)S_{or}\,, \tag{3.2.9}$$
$$\mathbf{k}^*_{r,owi} = f(\sigma^*)\mathbf{k}_{r,owi} + [1 - f(\sigma^*)]\,, \tag{3.2.10}$$
$$\mathbf{k}^*_{r,wor} = f(\sigma^*)\mathbf{k}_{r,wor} + [1 - f(\sigma^*)]\,, \tag{3.2.11}$$
$$a^* = f(\sigma^*)a + [1 - f(\sigma^*)]\,, \tag{3.2.12}$$
$$b^* = f(\sigma^*)b + [1 - f(\sigma^*)]\,. \tag{3.2.13}$$

The Corey's parameters modified are used to compute the new permeability curves.

We choose Corey's interpolation for its simplicity and because it is the most used in other works (Nielsen et al., 2010a; Amundsen, 2015) and it gives the result approaching those found by experiment.

Figure 3.2 shows the Corey's relative permeability curves for oil and water and the updated relative permeability curves.

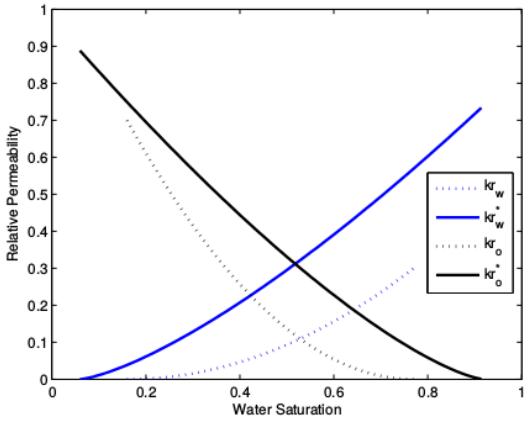

Figure 3.2: Corey' s interpolation method showing a new curve of relative permeability depending on IFT value with a=b=2, $s_{wi} = 0.16$ and $s_{or} = 0.23$ (Amundsen, 2015).

We observe in Figure 3.2 that the decrease of the water saturation causes the decrease of water relative permeability and hence causes the increase of oil saturation and oil relative permeability.

We can assume that the concentration of surfactant, which contributes to the change of IFT is that which is in water (Fulcher Jr et al., 1985; Shen et al., 2006). The ratio of concentration of surfactant in water M_{sw} and concentration of surfactant in oil M_{so} is

$$\frac{M_{sw}}{M_{so}} = \kappa \frac{S_w \rho_w}{S_o \rho_o}, \tag{3.2.14}$$

with $M_s = M_{sw} + M_{so}$, the total metabolites surfactant and κ the coefficient of partition. Therefore,

$$M_{sw} = \frac{M_s \kappa \frac{S_w \rho_w}{S_o \rho_o}}{1 + \kappa \frac{S_w \rho_w}{S_o \rho_o}}. \tag{3.2.15}$$

3.2.2 Polymer Modelling. The main role of the metabolites polymer is to increase the water dynamic viscosity. In Equation (3.2.2) of capillary number, we can remark that the increase of water viscosity contributes to the increase of capillary number, which is proportional to the enhancing of oil recovery. In fact, the increase of water viscosity slows the motion of the water, causing a great sweep of the zones where oil could be trapped. Moreover, the polymer has the property to adsorb through the thief zones. A thief zone is a region of high permeability where a fluid could leak instead of moving to the well of production. In fact, the adsorbed polymer will clog these thief zones and canalize oil through the well of recovery. An obstacle in this last role of polymer is that metabolites must be mixed for them to move quickly to these thief zones otherwise it will move slowly.

To find the value of viscosity for the mixed solution in the subsurface, one needs some experimentation and interpolation. Lacerda et al. (2012) use three different relations:

- **Linear relationship** which gives the updated value of water viscosity function of polymer concentration M_p in linear fashion,
$$\mu_w^* = \mu_w + GM_p\,, \tag{3.2.16}$$
where G is a constant.

- **Parabolic relationship** which gives a quadratic function. There are two relations found in previous works. The first relation comes from Lacerda et al. (2012)
$$\mu_w^* = 0.414M_p^2 + 1.895M_p + 0.071 \tag{3.2.17}$$
and the second comes from Bartelds et al. (1997) and takes into account the initial water viscosity
$$\mu_w^* = \mu_w[(5M_p)^2 + 5M_p + 1]\,. \tag{3.2.18}$$

- **Power law** which gives the updated water viscosity in the form
$$\mu_w^* = \mu_w + 1.4019M_p^{0.1653}\,. \tag{3.2.19}$$

Figure 3.3 has been done using Python to compare these four methods and select the most realistic.

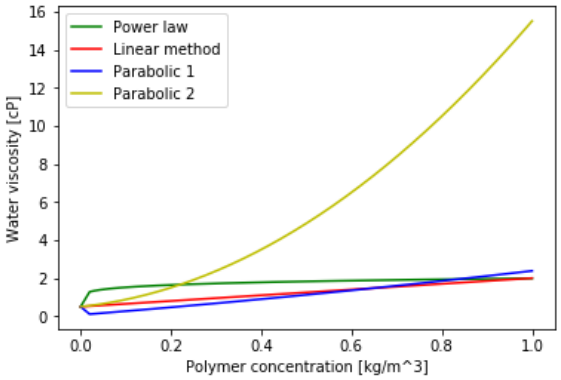

Figure 3.3: Influence of polymer concentration on water viscosity with $\mu_0 = 0.5$, and G=1.5

We can observe that power law is the most realistic because it ranges in admissible zones and starts by the increase of viscosity immediately after production of polymer. Also, we must take into account the time for polymer to mix in water. The current project will present a model proposed by Todd et al. (1972) and combines with the power law. The model will not only include the mixing parameter as presented by Todd et al. (1972), but it also considers the amount of adsorbed polymer concentration $M_{p,a}$ in the pores walls. The model has an assumption that the viscosity of a fully mixed polymer solution μ_m is a function of the total concentration polymer M_p. Therefore, the effective dynamic viscosity of polymer metabolite is a function of M_p i.e.,
$$\mu_p^* = \mu_m(M_p)^\omega \mu_p^{1-\omega}\,, \tag{3.2.20}$$
with $\omega \in \{0, 1\}$ a mixing parameter. For $\omega = 1$, the mixing is complete while for $\omega = 0$ there is no mixing. Todd et al. (1972) proposed the expression below for polymer velocity
$$\overrightarrow{u}_p = \frac{\mu_{w,misc}}{\mu_p^*}\overrightarrow{u}_w \tag{3.2.21}$$
$$= \left[(1-\bar{M}_p)\left(\frac{\mu_p}{\mu_w}\right)^{1-\omega} + \bar{M}_p\right]\overrightarrow{u}_w \tag{3.2.22}$$
$$= \mathcal{F}(\bar{M}_p)\overrightarrow{u}_w\,, \tag{3.2.23}$$

where $\bar{M}_p = \frac{M_p}{M_{p,max}}$ and $\mathcal{F}(\bar{M}_p) = (1-\bar{M}_p)\left(\frac{\mu_p}{\mu_w}\right)^{1-\omega} + \bar{M}_p$.

In previous works, the velocity of polymer was assumed to be equal to the water velocity. This assumption used in Amundsen (2015) led to the rejection of the adsorption of polymer. This simplifies the model but does not reach reality because by definition of biofilm, it is formed by an extracellular polymeric substance (EPS). In our case, we want to get the realistic model. For that, we will take into account that once polymer is produced, the water velocity changes and polymer moves at different velocity. Overall, we will neglect the polymer saturation, $S_p \approx 0$, since it is very small in the reservoir. The transport equation for polymer with adsorbed concentration $M_{p,a}$ is

$$\frac{\partial}{\partial t}\left(\frac{\phi S_w M_p}{\beta_w}\right) + \nabla.\left(\frac{\overrightarrow{u}_w M_{p,f}}{\beta_w} + \frac{\overrightarrow{u}_p M_{p,a}}{\beta_w}\right) = R_p\,. \tag{3.2.24}$$

The amount of adsorbed polymer concentration and free-floating polymer concentration $M_{p,f}$ is such that $M_p = M_{p,a} + M_{p,f}$ and it obeys Langmuir model with equilibrium for their partition as we will see in the next section.

Although surfactants and nutrients could adsorb, their effects have been neglected in other works (Volesky, 2003; Nielsen et al., 2010a). The effect of biofilm will be modelled in the next section.

3.3 Biofilm Modelling

Biofilm is a film produced by bacteria and polymer living in water. 95% of biofilm consists in an extracellular polymeric (EPS) caused by mixing of bacteria and polymer. This EPS is responsible of bioclogging (Thullner, 2010). The most common relationship used in adsorption cases is the Langmuir adsorption isotherm model with equilibrium. The kinetic derivation or Langmuir parameter (Masel, 1996) is

$$\mathcal{L} = \frac{w_1 w_2}{1 + w_1 w_2}\,, \tag{3.3.1}$$

where w_1 is the maximum attainable level of biofilm $[kg/m^2]$ or adsorbate's partial pressure and w_2 represents the speed of the absorption or the equilibrium constant. Therefore the adsorbed bacteria concentration B_a is

$$B_a = \mathcal{L}B\,, \tag{3.3.2}$$

and the free floating bacterial concentration is

$$B_f = B - B_a\,. \tag{3.3.3}$$

The biofilm repartition in this case, will take into account the adsorbed bacteria concentration and the adsorbed polymer concentration as shown in the following relation:

$$\psi = \frac{B_a}{\rho_b} + \frac{M_{p,a}}{\rho_b}\,, \tag{3.3.4}$$

where ρ_b represents the number of pore clogged by the biofilm. Neglecting $M_{p,a}$ as in Nielsen et al. (2010a) is a strong assumption. Here, we assume that the adsorbed polymer contributes also to the clogging of thief zones. After clogging, the rock propriety will change, the effective value of porosity becomes

$$\phi^* = \phi_0(1-\psi) = \phi_0\phi_{rel}\,, \tag{3.3.5}$$

with $\phi_{rel} = (1-\psi)$, the relative change of porosity and the updated water relative permeability is given by the empirical relation (Amundsen, 2015)

$$\mathbf{k}^*_{rw} = \mathbf{k}_{rw}\phi_{rel}^{19/6}\,. \tag{3.3.6}$$

With the inclusion of biofilm, the reaction terms become

$$\begin{aligned} R_b &= \eta_b(B_f + B_a)Y_b\,, && (3.3.7)\\ R_m &= \eta_m(B_f + B_a)Y_m\,, && (3.3.8)\\ R_n &= -R_b - R_m\,. && (3.3.9) \end{aligned}$$

A similar reasoning is applied for modelling adsorbed and free floating polymer using the Langmuir adsorption model. The index p, a is allocated to adsorbed polymer. The Langmuir parameter is

$$\alpha_{p,a} = \frac{w_{1p}w_{2p}}{1 + w_{1p}w_{2p}}\,, \tag{3.3.10}$$

with $M_{p,a} = \alpha_{p,a}M_p$.

3.4 Summary

The full model of microbial effect in oil recovery process is given by:

-Three velocities oil-water-polymer

$$\overrightarrow{u}_o = -\frac{\mathbf{k}_{r,o}}{\mu_o}\mathbf{k}(\nabla p_o - \rho_o\overrightarrow{g})\,, \tag{3.4.1}$$

$$\overrightarrow{u}_w = -\frac{\mathbf{k}_{r,w}}{\mu_w}\mathbf{k}(\nabla p_w - \rho_w\overrightarrow{g})\,, \tag{3.4.2}$$

$$\overrightarrow{u}_p = \mathcal{F}(\bar{M}_p)\overrightarrow{u}_w\,. \tag{3.4.3}$$

- The mass balance equations for oil, water and the transport equations for free floating-bacteria, adsorbed bacteria, surfactant, polymer (free floating and adsorbed) and nutrients are respectively

$$\begin{aligned} \frac{\partial}{\partial t}\left(\frac{\phi S_o}{\beta_o}\right) + \nabla.\left(\frac{\overrightarrow{u}_o}{\beta_o}\right) &= 0\,, && (3.4.4)\\ \frac{\partial}{\partial t}\left(\frac{\phi S_w}{\beta_w}\right) + \nabla.\left(\frac{\overrightarrow{u}_w}{\beta_w}\right) &= \widetilde{\mathbf{q}_w}\,, && (3.4.5)\\ \frac{\partial}{\partial t}\left(\frac{\phi S_w B_f}{\beta_w}\right) + \nabla.\left(\frac{\overrightarrow{u}_w B_f}{\beta_w}\right) &= \mathbf{q}_b + \eta_b B_f Y_b\,, && (3.4.6)\\ \frac{\partial}{\partial t}\left(\frac{\phi S_w B_a}{\beta_w}\right) &= \eta_b B_a Y_b\,, && (3.4.7)\\ \frac{\partial}{\partial t}\left(\frac{\phi S_w M_{sw}}{\beta_w}\right) + \nabla.\left(\frac{\overrightarrow{u}_w M_{sw}}{\beta_w}\right) &= R_s\,, && (3.4.8)\\ \frac{\partial}{\partial t}\left(\frac{\phi S_w M_p}{\beta_w}\right) + \nabla.\left(\frac{\overrightarrow{u}_w M_{p,f}}{\beta_w} + \frac{\overrightarrow{u}_p M_{p,a}}{\beta_w}\right) &= R_p\,, && (3.4.9)\\ \frac{\partial}{\partial t}\left(\frac{\phi S_w N}{\beta_w}\right) + \nabla.\left(\frac{\overrightarrow{u}_w N}{\beta_w}\right) &= \mathbf{q}_n + R_n\,, && (3.4.10) \end{aligned}$$

with $R_p + R_s = R_m$.

Equations (3.4.6) and (3.4.7) give a full model of Bacteria, and Equations (3.4.8) and (3.4.9) yield a full model of metabolites.

Any parameters in the equations above must be taken according to the expression with index * which give the expressions modified after microbial effect. Also, new values of porosity and water relative permeability must be updated according to the effect of biofilm (Equations (3.3.5) and (3.3.6)). We expect that the model given by Equations (3.4.1) up to (3.4.10) with all updated relations is the realistic model for microbial process even whether it is complicated.

For one dimension, the model leads to a system of six coupled Partial Differential Equations (PDEs). For oil, we have

$$\frac{\partial}{\partial t}\left(\frac{\phi S_o}{\beta_o}\right) - \frac{\partial}{\partial x}\left[\frac{\mathbf{k}_{r,o}\mathbf{k}}{\beta_o \mu_o}\left(\frac{\partial p_o}{\partial x} - \rho_o g\right)\right] = 0\,. \tag{3.4.11}$$

For water, we have

$$\frac{\partial}{\partial t}\left(\frac{\phi S_w}{\beta_w}\right) - \frac{\partial}{\partial x}\left[\frac{\mathbf{k}_{r,w}\mathbf{k}}{\beta_w \mu_w}\left(\frac{\partial p_w}{\partial x} - \rho_w g\right)\right] = \widetilde{\mathbf{q}_w}\,. \tag{3.4.12}$$

For bacteria, we have

$$\frac{\partial}{\partial t}\left(\frac{\phi S_w B}{\beta_w}\right) - \frac{\partial}{\partial x}\left[\frac{\mathbf{k}_{r,w}\mathbf{k}B}{\beta_w \mu_w (1 + w_1 w_2)}\left(\frac{\partial p_w}{\partial x} - \rho_w g\right)\right] = \mathbf{q}_b + \eta_{b,max}\frac{N}{K_b + N}BY_b\,. \tag{3.4.13}$$

For nutrients, we have

$$\frac{\partial}{\partial t}\left(\frac{\phi S_w N}{\beta_w}\right) - \frac{\partial}{\partial x}\left[\frac{\mathbf{k}_{r,w}\mathbf{k}N}{\beta_w \mu_w}\left(\frac{\partial p_w}{\partial x} - \rho_w g\right)\right] = \mathbf{q}_n - \eta_{b,max}\frac{N}{K_b + N}BY_b - \eta_{m,max}\frac{N - N_{crit}}{K_m + N - N_{crit}}BY_b\,. \tag{3.4.14}$$

For metabolites surfactant, we have

$$\frac{\partial}{\partial t}\left(\frac{\phi S_w M_s \kappa S_w \rho_w}{\beta_w (S_o \rho_o + \kappa S_w \rho_w)}\right) - \frac{\partial}{\partial x}\left[\frac{\mathbf{k}_{r,w}\mathbf{k}M_s \kappa S_w \rho_w}{\beta_w \mu_w (S_o \rho_o + \kappa S_w \rho_w)}\left(\frac{\partial p_w}{\partial x} - \rho_w g\right)\right] = \eta_{m,max}\frac{N - N_{crit}}{K_m + N - N_{crit}}BY_b\alpha_s\,. \tag{3.4.15}$$

For metabolite polymer, we have

$$\frac{\partial}{\partial t}\left(\frac{\phi S_w M_p}{\beta_w}\right) - \frac{\partial}{\partial x}\left[\frac{\mathbf{k}_{r,w}\mathbf{k}M_p}{\beta_w \mu_w}\left(\frac{\partial p_w}{\partial x} - \rho_w g\right)(\alpha_{p,f} + \mathcal{F}(\bar{M}_p)\alpha_{p,a})\right] = \eta_{m,max}\frac{N - N_{crit}}{K_m + N - N_{crit}}BY_b\alpha_p\,. \tag{3.4.16}$$

The coefficients α_p and α_s were used for the partition between surfactant and polymer such that $\alpha_p + \alpha_s = 1$ and also $\alpha_{p,f} = \alpha_p - \alpha_{p,a}$.

The assumptions in this model are as follows:

1. Diffusion is negligible.
2. The system is adiabatic and the fluctuations in temperature are negligible.
3. One dimension quasi-parallel fluid flow in a uniform porous medium.

4. Bacterial growth and metabolite production are modelled by Michaelis-Menten law and Monod model.
5. The valid model for absorbed bacteria and polymer is Langmuir model with equilibrium.
6. Only two kind of metabolites are produced - surfactant and polymer, other kinds are ignored.
7. Bacteria, nutrients and surfactants are dispersed in water and their distributions are instantaneous.
8. The amount of surfactant in oil does not have an effect.
9. Polymer modifies the velocity of water and hence flows at different velocity.
10. Biofilm created by bacteria stick on thief zones and has a null velocity.
11. Indigenous bacteria is ignored.
12. Any bacterial reproduction or metabolite production in biofilm is introduced in water.
13. Chemotaxis does not occur.
14. Only bacteria and polymer adsorb.
15. Oil and water could be compressible.

Further, other assumptions may be used on this model for small implementation. But until now, To the best of our knowledge, there is no analytical solution for the model above. A numerical method must be used.

4. Discretization and simulation

Partial differential equations which cannot be solved by analytical methods are usually approximated using numerical methods. In this work, for the spatial discretization, we use finite volume methods (FVMs) with cell-centred. This method is the used in approximation of the solution for many physical problems, especially in fluid dynamics (LeVeque, 2002; Griebel et al., 1998). In this Chapter, we will present the dicretization of the full model presented in the previous chapter. Because of the complexity of the model, the implementation will be done in Python using the model of lines (MOL). This means that we will only descretize the space and transform the time derivative in an ordinary differential equation. In addition, we will use some assumptions on the full model.

4.1 Time Discretization

Looking at the equations we have obtained, we start with time discretization. For that, we use vertex centered grid in 1D, from an intial time t_0 to a final time t_N. The time step $\triangle t = h$ is uniform for all steps. For a partial differential equation of the form

$$u_t(x,t) = F(u,t)\,, \tag{4.1.1}$$

there are different methods used to approximate the solution. In this work, we use the Implicit Euler method because it is more stable then other methods (Landa Marban, 2016), therefore, Equation (4.1.1) gives

$$u^{k+1} = u^k + F(u^{k+1}, t^{k+1})\triangle t + O(\triangle t^2)\,. \tag{4.1.2}$$

4.2 Space Discretization

The space discretization is done in 1D. Let us consider the domain Ω partitioned in many small control volume Ω_i so that $x_i = x_0 + i\triangle x$ with $\triangle x$ the uniform length for every piece of the mesh. The volume control is such that $\Omega = \cup_{i=1}^{r}\Omega_i$ with r the number of piecewise. The aim of space discretization is to find a numerical solution of our problem in the points $\{x_i\}$. For that we use the cell-centered grid in 1D as shown in Figure 4.1.

For one dimension, Ω_i is an interval such that $\Omega_i = [x_{i-\frac{1}{2}}, x_{i+\frac{1}{2}})$. Let the length of the cell i be such that $x_{i+\frac{1}{2}} - x_{i-\frac{1}{2}} = \xi$ is uniform for all $i \in [1, r]$. Hence, $\xi = \frac{x_n - x_0}{r} = \triangle x$.

4.2.1 Approximation of derivatives. From Taylor expansion (Canuto and Tabacco, 2011), we deduce

$$\left(\frac{\partial u}{\partial x}\right)_i = \frac{u_{i+1} - u_i}{\xi} + O(\xi) \qquad \text{Forward difference}\,, \tag{4.2.1}$$

$$\left(\frac{\partial u}{\partial x}\right)_i = \frac{u_i - u_{i-1}}{\xi} + O(\xi) \qquad \text{Backward difference}\,, \tag{4.2.2}$$

$$\left(\frac{\partial u}{\partial x}\right)_i = \frac{u_{i+\frac{1}{2}} - u_{i-\frac{1}{2}}}{\xi} + O(\xi^2) \qquad \text{centred diffusion}\,, \tag{4.2.3}$$

where $u_{-\frac{1}{2}}$ or $u_{r+\frac{1}{2}}$ are unavailable. Equations (4.2.1) and (4.2.2) are used on the boundary.

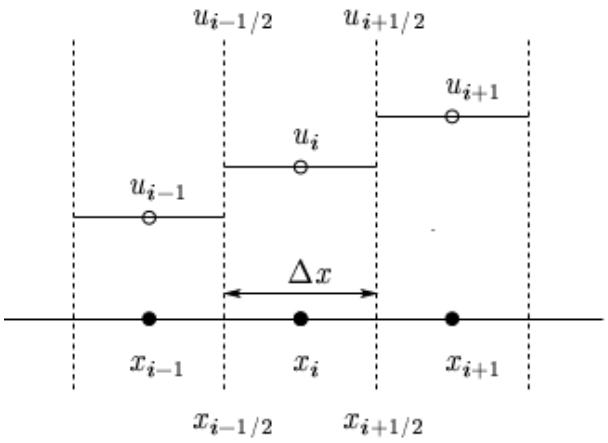

Figure 4.1: Piecewise-constant (Griebel et al., 1998).

4.2.2 Approximation of integral. Using the midpoint rule and the numerical integration, we can approximate the integral for a cell-centered grid (Landa Marban, 2016) by

$$\int_{\Omega_i} f(x) d\Omega_i \approx |\Omega_i| f_i \,, \tag{4.2.4}$$

where f_i is the value of the flux function $f(x)$ on the midpoint of Ω_i and $|\Omega_i| = \triangle x = \xi$ the length of Ω_i.

4.2.3 Two-point flux approximation. In our model, if we ignore the part of time variation, we end up with a model of the form

$$-\nabla.(c\nabla y) = F \,. \tag{4.2.5}$$

The idea is to find the value of y. In finite difference, the operator derivatives are replaced by the differences between discrete sets of points in a domain. But finite volume methods consider the law of mass conservation over adjacent cell volumes (Aarnes et al., 2007). Integration of Equation (4.2.5) on Ω_i gives

$$-\int_{\Omega_i} \nabla.(c\nabla y) d\xi = \int_{\Omega_i} F d\xi \,. \tag{4.2.6}$$

Using the Divergence Theorem, we get

$$-\int_{\partial\Omega_i} c(\nabla y.\overrightarrow{n}) dS = \int_{\Omega_i} F d\xi \,. \tag{4.2.7}$$

The left side of Equation (4.2.7) is computed at the boundary of Ω_i. In 1D, we have two boundaries $\gamma_{i+1} = \Omega_{i+1} \cap \Omega_i$ and $\gamma_i = \Omega_i \cap \Omega_{i-1}$. Therefore, the gradient of y will be obtained using two-point flux approximation i.e., using a current cell and one of its adjacent cell such that

$$\nabla y \approx \frac{y_i - y_{i-1}}{\xi} \qquad \text{on } \gamma_i \,. \tag{4.2.8}$$

For both boundaries, Equation (4.2.7) gives

$$-\left(\frac{y_{i+1} - y_i}{\xi}\bar{c}_i - \frac{y_i - y_{i-1}}{\xi}\bar{c}_{i-1}\right) = \bar{F}\xi \,, \tag{4.2.9}$$

where $\bar{c}$ is the approximation of parameter c on the boundary as explained in the next section.

4.2.4 Approximation of the parameter on the integral boundaries. Many techniques exist for the approximation of a parameter c on the boundaries depending on the nature of the parameter (Aziz and Settari, 1979). We will use, for conformity and simplicity, the upstream weighting method (Chen et al., 2006)

$$c_{i+\frac{1}{2}} \approx c_i \,, \tag{4.2.10}$$

$$c_{i-\frac{1}{2}} \approx c_{i-1} \,. \tag{4.2.11}$$

4.2.5 Time and discretization of an equation model. For example, let us consider a PDE below which seems like one of the equations that we have obtained in the model (previous chapter):

$$\frac{\partial}{\partial t} g - \frac{\partial}{\partial x}\left[G(g,x,t)(\frac{\partial f}{\partial x} - v)\right] = F(t,x)\,, \tag{4.2.12}$$

where $F(t,x)$ represents the function source term, $G(g,x,t)$ represents the parameter function, g represents the flux function, f represents the pressure and v represents the gravitation force. Let us assume that i is the index of the centre of the cell such that $i-\frac{1}{2}$ and $i+\frac{1}{2}$ represents respectively the left and the right boundaries, and k is the index related to the time. With all the consideration above, the basic form of numerical schemes for a particular j component is

$$\begin{aligned}\frac{1}{h}\left[g_{j,i}^{k+1} - g_{j,i}^{k}\right] - \frac{1}{\xi}\left(G(g,x,t)_{j,i}^{k+1}\right)\left[\frac{1}{\xi}\left((f)_{j,i+1}^{k+1} - (f)_{j,i}^{k+1}\right) - v_{j,i}^{k+1}\right] + \\ \frac{1}{\xi}\left(G(g,x,t)_{j,i-1}^{k+1}\right)\left[\frac{1}{\xi}\left((f)_{j,i}^{k+1} - (f)_{j,i-1}^{k+1}\right) - v_{j,i-1}^{k+1}\right] = \bar{F}_{j,i}^{k+1}\,.\end{aligned} \tag{4.2.13}$$

4.3 Discretization of the Full Model

A similar reasoning, from Equation (4.2.13), applied on the model obtained in the previous chapter yields the discretization below. For oil, we have

$$\begin{aligned}\frac{\xi^2}{h}\left[\left(\rho_o S_o \phi\right)_i^{k+1} - \left(\rho_o S_o \phi\right)_i^{k}\right] - \left(\frac{\mathbf{k}_{r,o}\mathbf{k}\rho_o}{\mu_o}\right)_i^{k+1}\left[(p_o)_{i+1}^{k+1} - (p_o)_i^{k+1} - \xi(\rho_o g)_i^{k+1}\right] + \\ \left(\frac{\mathbf{k}_{r,o}\mathbf{k}\rho_o}{\mu_o}\right)_{i-1}^{k+1}\left[(p_o)_i^{k+1} - (p_o)_{i-1}^{k+1} - \xi(\rho_o g)_{i-1}^{k+1}\right] = 0\,.\end{aligned} \tag{4.3.1}$$

For water, we have

$$\begin{aligned}\frac{\xi^2}{h}\left[\left(\rho_w S_w \phi\right)_i^{k+1} - \left(\rho_w S_w \phi\right)_i^{k}\right] - \left(\frac{\mathbf{k}_{r,w}\mathbf{k}\rho_w}{\mu_w}\right)_i^{k+1}\left[(p_w)_{i+1}^{k+1} - (p_w)_i^{k+1} - \xi(\rho_w g)_i^{k+1}\right] + \\ \left(\frac{\mathbf{k}_{r,w}\mathbf{k}\rho_w}{\mu_w}\right)_{i-1}^{k+1}\left[(p_w)_i^{k+1} - (p_w)_{i-1}^{k+1} - \xi(\rho_w g)_{i-1}^{k+1}\right] = \xi^2\left(\mathbf{q}_w\right)_i^{k+1}\,.\end{aligned} \tag{4.3.2}$$

For bacteria, we have

$$\begin{aligned}\frac{\xi^2}{h}\left[\left(\frac{\rho_w S_w \phi B}{\beta_w}\right)_i^{k+1} - \left(\frac{\rho_w S_w \phi B}{\beta_w}\right)_i^{k}\right] - \\ \left(\frac{\mathbf{k}_{r,w}\mathbf{k}B}{\beta_w \mu_w (1+w_1 w_2)}\right)_i^{k+1}\left[(p_w)_{i+1}^{k+1} - (p_w)_i^{k+1} - \xi(\rho_w g)_i^{k+1}\right] + \\ \left(\frac{\mathbf{k}_{r,w}\mathbf{k}B}{\beta_w \mu_w (1+w_1 w_2)}\right)_{i-1}^{k+1}\left[(p_w)_i^{k+1} - (p_w)_{i-1}^{k+1} - \xi(\rho_w g)_{i-1}^{k+1}\right] = \\ \xi^2\left(\mathbf{q}_b + \eta_{b,max}\frac{N}{K+N}BY_b\right)_i^{k+1}.\end{aligned} \tag{4.3.3}$$

For nutrients, we have

$$\begin{aligned}\frac{\xi^2}{h}\left[\left(\frac{\rho_w S_w \phi N}{\beta_w}\right)_i^{k+1} - \left(\frac{\rho_w S_w \phi N}{\beta_w}\right)_i^{k}\right] - \\ \left(\frac{\mathbf{k}_{r,w}\mathbf{k}N}{\beta_w \mu_w}\right)_i^{k+1}\left[(p_w)_{i+1}^{k+1} - (p_w)_i^{k+1} - \xi(\rho_w g)_i^{k+1}\right] + \\ \left(\frac{\mathbf{k}_{r,w}\mathbf{k}N}{\beta_w \mu_w}\right)_{i-1}^{k+1}\left[(p_w)_i^{k+1} - (p_w)_{i-1}^{k+1} - \xi(\rho_w g)_{i-1}^{k+1}\right] = \\ \xi^2\left(\mathbf{q}_n - \eta_{b,max}\frac{N}{K_b+N}BY_b - \eta_{m,max}\frac{N-N_{crit}}{K+N-N_{crit}}BY_b\right)_i^{k+1}.\end{aligned} \tag{4.3.4}$$

For metabolites surfactant, we have

$$\begin{aligned}\frac{\xi^2}{h}\left[\left(\frac{\rho_w S_w \phi M_s \kappa S_w \rho_w}{\beta_w (S_o\rho_o + \kappa S_w \rho_w)}\right)_i^{k+1} - \left(\frac{\rho_w S_w \phi M_s \kappa S_w \rho_w}{\beta_w (S_o\rho_o + \kappa S_w \rho_w)}\right)_i^{k}\right] - \\ \left(\frac{\mathbf{k}_{r,w}\mathbf{k}M_s \kappa S_w \rho_w}{\beta_w \mu_w (S_o\rho_o + \kappa S_w \rho_w)}\right)_i^{k+1}\left[(p_w)_{i+1}^{k+1} - (p_w)_i^{k+1} - \xi(\rho_w g)_i^{k+1}\right] + \\ \left(\frac{\mathbf{k}_{r,w}\mathbf{k}M_s \kappa S_w \rho_w}{\beta_w \mu_w (S_o\rho_o + \kappa S_w \rho_w)}\right)_{i-1}^{k+1}\left[(p_w)_i^{k+1} - (p_w)_{i-1}^{k+1} - \xi(\rho_w g)_{i-1}^{k+1}\right] = \\ \xi^2\left(\eta_{m,max}\frac{N-N_{crit}}{K+N-N_{crit}}BY_b\alpha_s\right)_i^{k+1}.\end{aligned} \tag{4.3.5}$$

For metabolite polymer, we have

$$\begin{aligned}\frac{\xi^2}{h}\left[\left(\frac{\rho_w S_w \phi M_p}{\beta_w}\right)_i^{k+1} - \left(\frac{\rho_w S_w \phi M_p}{\beta_w}\right)_i^{k}\right] - \\ \left(\frac{\mathbf{k}_{r,w}\mathbf{k}M_p}{\beta_w \mu_w}(\alpha_{p,f} + \mathcal{F}(\bar{M}_p)\alpha_{p,a})\right)_i^{k+1}\left[(p_w)_{i+1}^{k+1} - (p_w)_i^{k+1} - \xi(\rho_w g)_i^{k+1}\right] + \\ \left(\frac{\mathbf{k}_{r,w}\mathbf{k}M_p}{\beta_w \mu_w}(\alpha_{p,f} + \mathcal{F}(\bar{M}_p)\alpha_{p,a})\right)_{i-1}^{k+1}\left[(p_w)_i^{k+1} - (p_w)_{i-1}^{k+1} - \xi(\rho_w g)_{i-1}^{k+1}\right] = \\ \xi^2\left(\eta_{m,max}\frac{N-N_{crit}}{K+N-N_{crit}}BY_b\alpha_p\right)_i^{k+1}.\end{aligned} \tag{4.3.6}$$

4.4 Initial and Boundary Conditions

The solution of a differential equation gives an infinte number of solutions. To have a particular solution, we must fix the conditions at time t_0, called initial conditions, and the values at the boundaries of the volume control Ω_i called boundary conditions. The boundary conditions in this context satisfy the Dirichlet conditions (values given on boundaries), $X(x,t_0) = h(x,t_0)$, with $x \in \partial\Omega_i$, the Neumann conditions (normal derivative is given on the boundary), $\frac{\partial X(x,t_0)}{\partial n} = l(x,t_0)$, with $x \in \partial\Omega_i$ and the flux conditions (the flux is given on the boundary). The Tables 1, 2 and 3 in appendix contain the initials conditions and boundary conditions which are used in this current project.

4.5 Simulation of a Simplified MEOR Model

There is an open source code developed by The Foundation for Scientific and Industrial Research (SINTEF) (Lie, 2014) called Matlab Reservoir Simulation Toolbox (MRST) for simulation of reservoirs problems. The implementation for such a discretized model found in the previous section will take more time than it allocated for this current project. However, to get the idea on the advantages of MEOR process, we will use some assumptions on the realistic model. The aim is to change the PDE to an ODE for a particular fixed time t_k. For that we use the Method of lines (MOR) with only discretization of space and the dependant in time will be total. As assumptions, we will neglect the effect of capillary pressure, gravity force, biofilm and consider that only surfactant is the metabolite produced as assumed in some work (Nielsen et al., 2010a) and moreover surfactant remain only in water.

4.5.1 Weak MEOR Model. Considering the above assumptions, Equations (3.1.6), (3.1.7), (3.1.8), (3.1.9), (4.1.1), (3.1.10) in 1D lead to:

$$\frac{\partial}{\partial t}\phi S_o - \frac{\partial}{\partial x}\left(\lambda_o \frac{\partial p}{\partial x}\right) = 0\,, \tag{4.5.1}$$

$$\frac{\partial}{\partial t}\phi S_w - \frac{\partial}{\partial x}\left(\lambda_w \frac{\partial p}{\partial x}\right) = \frac{q_w}{\rho_w}\,, \tag{4.5.2}$$

$$\frac{\partial}{\partial t}\phi B S_w - \frac{\partial}{\partial x}\left(\lambda_w B \frac{\partial p}{\partial x}\right) = q_b + R_b\,, \tag{4.5.3}$$

$$\frac{\partial}{\partial t}\phi N S_w - \frac{\partial}{\partial x}\left(\lambda_w N \frac{\partial p}{\partial x}\right) = q_n + R_n\,, \tag{4.5.4}$$

$$\frac{\partial}{\partial t}\phi M S_w - \frac{\partial}{\partial x}\left(\lambda_w M \frac{\partial p}{\partial x}\right) = +R_m\,, \tag{4.5.5}$$

where $\lambda_o = \frac{\mathbf{k}_{r,o}}{\mu_o}\mathbf{k}$ and $\lambda_w = \frac{\mathbf{k}_{r,w}}{\mu_o}\mathbf{k}$. These relations are of the form

$$\frac{\partial}{\partial t}g - \frac{\partial}{\partial x}[G(g,x,t)(\frac{\partial f}{\partial x})] = F(t,x)\,. \tag{4.5.6}$$

The discretization of Equation (4.5.6) in space at fixed time t_k for a component j gives

$$\frac{dg_j}{dt} = \frac{1}{\xi}\Big(G(g,x,t)_{j,i}\Big)\left[\frac{1}{\xi}\Big((f)_{j,i+1} - (f)_{j,i}\Big)\right] - \frac{1}{\xi}\Big(G(g,x,t)_{j,i-1}\Big)\left[\frac{1}{\xi}\Big((f)_{j,i} - (f)_{j,i-1}\Big)\right] + F_{j,i}\,. \tag{4.5.7}$$

The same reasoning, from Equation (4.5.7), will be used on the weak model above.

Adding Equation (4.1.2) and Equation (4.5.1), we get after discretization

$$-\frac{1}{\xi}\lambda_{t,i}\frac{1}{\xi}\Big(p_{i+1}-p_i\Big)+\frac{1}{\xi}\lambda_{t,i-1}\frac{1}{\xi}\Big(p_i-p_{i-1}\Big)=\frac{q_{w,i}}{\rho_w}\,, \tag{4.5.8}$$

with $\lambda_t=\lambda_w+\lambda_o$. The same, discretization on (4.5.1), (4.5.2), (4.5.3) and (4.5.4) gives

$$\frac{dS_w}{dt}=\frac{1}{\phi}\Big[\frac{q_{w,i}}{\rho_w}+\frac{1}{\xi}\lambda_{w,i}\frac{1}{\xi}\Big(p_{i+1}-p_i\Big)-\frac{1}{\xi}\lambda_{w,i-1}\frac{1}{\xi}\Big(p_i-p_{i-1}\Big)\Big] \tag{4.5.9}$$

$$\frac{dB}{dt}=\frac{1}{S_w}\Big\{\frac{1}{\phi}\Big[q_{b,i}+R_{b,i}+\frac{1}{\xi}B_i\lambda_{w,i}\frac{1}{\xi}\Big(p_{i+1}-p_i\Big)-\frac{1}{\xi}B_{i-1}\lambda_{w,i-1}\frac{1}{\xi}\Big(p_i-p_{i-1}\Big)\Big]-B\frac{dS_w}{dt}\Big\} \tag{4.5.10}$$

$$\frac{dN}{dt}=\frac{1}{S_w}\Big\{\frac{1}{\phi}\Big[q_{n,i}+R_{n,i}+\frac{1}{\xi}N_i\lambda_{w,i}\frac{1}{\xi}\Big(p_{i+1}-p_i\Big)-\frac{1}{\xi}N_{i-1}\lambda_{w,i-1}\frac{1}{\xi}\Big(p_i-p_{i-1}\Big)\Big]-N\frac{dS_w}{dt}\Big\} \tag{4.5.11}$$

$$\frac{dM}{dt}=\frac{1}{S_w}\Big\{\frac{1}{\phi}\Big[R_{m,i}+\frac{1}{\xi}B_i\lambda_{w,i}\frac{1}{\xi}\Big(p_{i+1}-p_i\Big)-\frac{1}{\xi}M_{i-1}\lambda_{w,i-1}\frac{1}{\xi}\Big(p_i-p_{i-1}\Big)\Big]-M\frac{dS_w}{dt}\Big\} \tag{4.5.12}$$

Equations (4.5.8), (4.5.9), (4.5.10), (4.5.11) and (4.5.12) constitute a system of the form:

$$\begin{cases}\frac{d\bar{U}}{dt}=f(\bar{U},t)\,,\\ U_1=f_2(\bar{U},t)\,,\\ \bar{U}(0)=\bar{U}_0\,,\end{cases} \tag{4.5.13}$$

where the vector of unknown is $\bar{U}^T=(S_w,B,N,M)$ and U_1 is the pressure.

4.5.2 Implementation. The implementation of the ODE above will be done using Python Software. For evolution of concentration of bacteria, nutrients and metabolites in time, and water saturation we have the Figure 4.2. The simulation is done using a cell length of 4m for a fixed time of 10 days. We observe

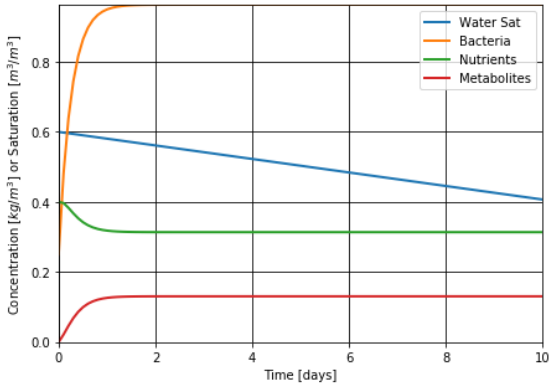

Figure 4.2: Evolution of bacteria, nutrients and metabolites concentration and water saturation in the first cell.

that, bacteria consume nutrients and produce metabolites. But these productions and depletion remain constant as time goes on. The reason that is there is always an amount of bacteria and nutrients injected each day in terms of source term. The implementation is done for water volume flux of $80kg/m^3day$. Also we observe that water saturation starts decreasing linearly after the production of the metabolites.

Figure 4.3 presents the evolution of relative permeability curves and the evolution of the IFT in the first cell. IFT slows done very quickly allowing oil to be produced. The consequence of this is the increase of oil relative permeability curve.

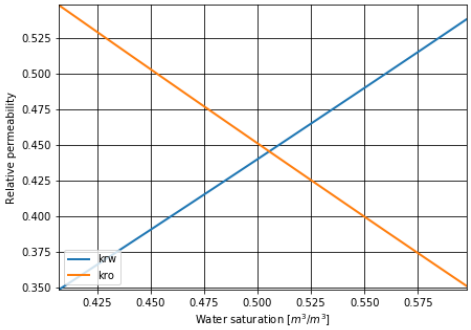

(a) Relative permeability curves.

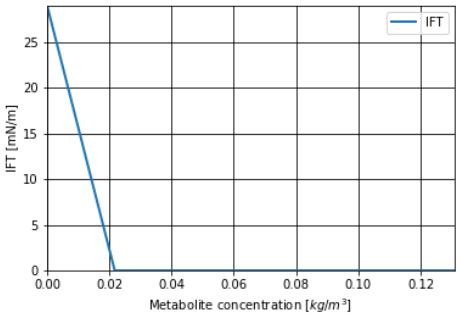

(b) IFT.

Figure 4.3: Evolution of relative permeability curves in the first cell

The process of MEOR could be compared with a simple water flooding process under the same variation of pressure. The aim is to see the evolution of oil recovery. For that, we can compute the oil recovered by

$$\text{oil recovery} = u_o A t\,, \tag{4.5.14}$$

where t is the time and A the cross-sectional area. The OIIP is given by

$$\%\text{OIIP} = (\text{oil recovery/oil initially in place}) \times 100\,. \tag{4.5.15}$$

For a volume control of $V = A.L$, the initial oil is $V_o = \phi V S_o$, with L the length of the domain. Figure 4.4 shows that MEOR process could produce up to 85% of OIIP while a water flooding could produce just 10% for the same amount of water injected. In Nielsen et al. (2010a), MEOR process produce 79% of OIIP while in Amundsen (2015) it is 71%.

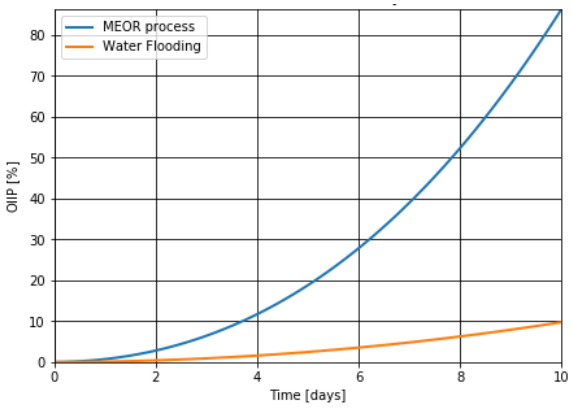

Figure 4.4: Evolution in time for water and oil saturation.

In Figure 4.5, the pressure is decreasing parabolically as expected from its PDE. The initial pressure starts by $10^7\ Pa$ and ends up with $10^7 - 50\ Pa$ for 200m.

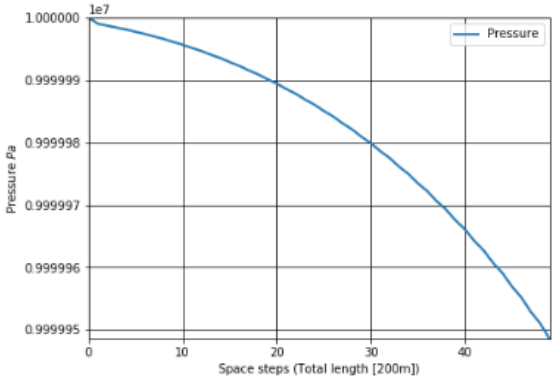

Figure 4.5: Pressure for 200m.

4.6 Summary

In this chapter, we used the Finite Volume Method for the discretization in space of the model found in previous chapter. The space and time discretization used is 1D. The simulation presented, have been implemented using Python software for the simplified MEOR model (with only surfactant effect). The results show that MEOR could produce up to 85% of OIIP for in the first cell, while in the same conditions a simple water flooding produce 10%. However, the effect of surfactant is very visible because with $0.02 kg/m^3$ of concentration, the IFT is reduced to $0 mN/m$ and the pressure is reduced with $50 Pa$ for a length of $200 m$.

5. Conclusion

In this work we provided a full realistic model of microbial effect in enhancing oil recovery. The model yielded a system of six partial differential equations which reflect the mass balance. Water and oil have been modelled as two phase flow in a porous medium. Other substances are assumed to be transported in water. The model of growth rate and depletion of biological substances were done using Michaelis-Menten kinetic and Monod models. For the change of relative permeability due to the effect of surfactant, we have adopted Corey model. Moreover, the power law was the best model for the change of water viscosity due to polymer effect. However, there is an extracellular produced by both adsorbed bacteria and polymer called biofilm. It was done using Langmuir with equilibrium model for adsorption. This biofilm clogs thief zones and changes the rock properties.

In Chapter 4, a discretization in one dimension using Finite Volume Methods with vertex-centered was used for numerical method. The implementation was done using other assumptions to display the meaningful effect of microbial method only with surfactant. The results have shown that the effect of surfactant could produce 85% of the OIIP. Under the same conditions, a simple flooding process could only give 10% of the OIIP.

The global implementation of the model done in this work could be the subject of a future research. We hope that the result will be closer to the reality and the industries will get a decision tool from this work. Other future works could also consider the effect of "fracturing" in microbial process and the effect of diffusion.

Appendix List of Symbols

Symbol	Initial Value	Unit	Description
α			Langmuir symbol for polymer
a, b	2	-	Corey's exponents
B	0.25	kg/m^3	Bacteria concentration
B_a		kg/m^3	Adsorbed bacteria concentration
B_f		kg/m^3	Concentration of free-floating bacteria
c	-	kg/m^3	Concentration
h		$days$	Time scale
κ	-	-	Coefficient of partition for surfactant
K_b	0.5	kg/m^3	Substrate concentration for half growth rate of bacteria
K_m	0.7	kg/m^3	Substrate concentration for half growth rate of Metabolites
$\mathbf{k}$	[100]	mD	Absolute permeability tensor
$\mathbf{K}$	100	mD	Absolute permeability
$\mathbf{k}_{ro}$		-	Oil relative permeability
$\mathbf{k}_{rw}$		-	Water relative permeability
$\mathbf{k}_{r,owi}$	0.7	-	Oil relative permeability at initial water saturation
$\mathbf{k}_{r,wor}$	0.3	-	Water relative permeability residual oil saturation
$\mathbf{k}_{rw,base}$		-	Basic water relative permeability
$\mathbf{k}_{ro,base}$		-	Basic oil relative permeability
$\mathbf{k}_{rw,misc}$		-	Miscible water relative permeability
$\mathbf{k}_{ro,misc}$		-	Miscible oil relative permeability
l_1, l_2, l_3	$\{10^{-4}, 0.2, 1.510^4\}$	-	Parameters for surfactant effect
$\mathcal{L}$			Langmuir symbol for bacteria
M	0	kg/m^3	Metabolite concentration
M_s	0	kg/m^3	Metabolite surfactant concentration
M_{sw}		kg/m^3	Surfactant concentration in water
M_{so}		kg/m^3	Surfactant concentration in oil
M_p	0	kg/m^3	Metabolite polymer concentration
$M_{p,a}$		kg/m^3	Concentration of adsorbed polymer
$M_{p,max}$		kg/m^3	Maximum effective concentration of polymer
$\bar{M}_p$		-	Ratio of $M_p/M_{p,max}$
N	0.4	kg/m^3	Nutrient concentration
N_{crit}	0.01	kg/m^3	Critical nutrient concentration for metabolite production
N_{ca}		-	Capillary number
ω		-	Mixing parameter
Ω		-	Arbitrarily domain
p	10^7	Pa	Total pressure
p_o		Pa	Partial pressure in oil
p_w		Pa	Partial pressure in water
p_c		Pa	Capillary pressure

Table 1: Appendix A (Romero-Zerón, 2012; Yen, 1989; Nielsen et al., 2010a; Amundsen, 2015)

Symbol	Initial Value	Unit	Description
ψ		-	Biofilm repartition
$\mathbf{q}_b$	0.65	kg/m^3day	Bacteria source term
$\mathbf{q}_n$	0.05	kg/m^3day	Nutrient source term
$\mathbf{q}_o$	0	kg/m^3day	Oil source term
$\mathbf{q}_w$	80	kg/m^3day	Water source term
$\widetilde{\mathbf{q}}_o$		day^{-1}	Source term altered by compressibility of injected oil
$\widetilde{\mathbf{q}}_w$		day^{-1}	Source term altered by compressibility of injected water
R_b		kg/m^3day	Bacteria reaction term
R_m		kg/m^3day	Metabolites reaction term
R_n		kg/m^3day	Nutrient reaction term
r_{eff}		m	Effective radius curvature of the pore
S_o	0.4	m^3/m^3	Oil saturation
S_w	0.6	m^3/m^3	Water saturation
S_{or}	0.23	m^3/m^3	Residual oil saturation
S_{wi}	0.16	m^3/m^3	Initial water saturation
$\overrightarrow{u}_o$		m/day	Oil velocity
$\overrightarrow{u}_w$		m/day	Water velocity
$\overrightarrow{u}_m$		m/day	Metabolite velocity
$\overrightarrow{u}_p$		m/day	Polymer velocity
V		m^3	Elementary volume
Y_b	0.3	-	Bacteria yield coefficient
Y_m	0.7	-	Metabolite yield coefficient
β_o	1	-	Oil volume factor
β_w	1	-	Water volume factor
μ_o	5	cP	Oil dynamic viscosity
μ_w	1	cP	Water dynamic viscosity
μ_p		cP	Polymer dynamic viscosity
ϵ	6	-	Coats's exponent for interpolation
η_b		day^{-1}	Growth rate of bacteria
$\eta_{b,max}$	0.2	day^{-1}	Maximum growth rate of bacteria
η_m		day^{-1}	Production rate of metabolite
$\eta_{m,max}$	0.6	day^{-1}	Maximum production rate of metabolite
ρ_b		kg/m^3	number of pores clogged by biofilm
ρ_o	800	kg/m^3	Oil density
ρ_w	1000	kg/m^3	Water density
$\rho_{sc,o}$	800	kg/m^3	Oil density at surface conditions
$\rho_{sc,w}$	1000	kg/m^3	Water density at surface conditions
σ	29	mN/m	Interfacial tension
τ		-	Tortuosity
τ_c		cP	Dynamic capillary
θ	-	rad	Angle between pore surface and interface water-oil

Table 2: Appendix A (Romero-Zerón, 2012; Yen, 1989; Nielsen et al., 2010a; Amundsen, 2015)

Symbol	Initial Value	Unit	Description
ϕ	0.4	-	Porosity
ξ		m	Length scale
ω_1		kg/m^2	Langmuir distribution parameter
ω_2		kg/m^3	Langmuir distribution parameter
*	-	-	Superscript for new property value
0	-	-	Subscript for initial property value

Table 3: Appendix C (Romero-Zerón, 2012; Yen, 1989; Nielsen et al., 2010a; Amundsen, 2015)

Acknowledgements

I thank the almighty God for allowing me to finish this work on time..

My thanks go also to AIMS staff (Prof Neil Geoffrey Turok, Prof Barry Green and Prof J. Sanders) for their warm coaching and having provided a higher quality education center to young Africans.

I am very grateful of Dr Antoine Tambue for having easily accepted to supervise this work and for his helpful advices. This topic given to me by himself has been a better source of knowledge in my field. His coach gave me the taste to continue in the research.

I will be ungrateful if I will not thank Mr Eyaya Birara for his advices and Mrs Noluvoyo Hobana for her assistance in the correction of English grammar.

References

J. E. Aarnes, T. Gimse, and K.-A. Lie. An introduction to the numerics of flow in porous media using matlab. In *Geometric modelling, numerical simulation, and optimization*, pages 265–306. Springer, 2007.

A. Amundsen. Microbial enhanced oil recovery-modeling and numerical simulations. Master's thesis, NTNU, 2015.

K. Aziz and A. Settari. *Petroleum reservoir simulation*. Chapman & Hall, 1979.

I. M. Banat, R. S. Makkar, and S. S. Cameotra. Potential commercial applications of microbial surfactants. *Applied microbiology and biotechnology*, 53(5):495–508, 2000.

G. Bartelds, J. Bruining, and J. Molenaar. The modeling of velocity enhancement in polymer flooding. *Transport in Porous Media*, 26(1):75–88, 1997.

P. Bastian. *Numerical computation of multiphase flows in porous media*. Phd, Christian Albrech universitet Germany, 1999.

C. Canuto and A. Tabacco. *Mathematical analysis II*. Springer Science & Business Media, 2011.

Z. Chen, G. Huan, and Y. Ma. *Computational methods for multiphase flows in porous media*. SIAM, 2006.

M. Destefanis and G. Savioli. Influence of relative permeabilities on chemical enhanced oil recovery. In *Journal of Physics: Conference Series*, volume 296, page 012014. IOP Publishing, 2011.

A. G. Eldeen, A. M. A. A. Alhadi, and M. A. Mergani. Microbial Enhanced Oil Recovery (MEOR). Master's thesis, University of Khartoum, 2013.

J. R. Fanchi. *Principles of applied reservoir simulation*. Gulf Professional Publishing, 2005.

R. A. Fulcher Jr, T. Ertekin, C. Stahl, et al. Effect of capillary number and its constituents on two-phase relative permeability curves. *Journal of petroleum technology*, 37(02):249–260, 1985.

M. Griebel, T. Dornseifer, and T. Neunhoeffer. *Numerical simulation in fluid dynamics: a practical introduction*. SIAM, 1998.

S. M. Hassanizadeh, M. A. Celia, and H. K. Dahle. Dynamic effect in the capillary pressure–saturation relationship and its impacts on unsaturated flow. *Vadose Zone Journal*, 1(1):38–57, 2002.

H. E. Huppert and J. A. Neufeld. The fluid mechanics of carbon dioxide sequestration. *Annual review of fluid mechanics*, 46:255–272, 2014.

M. Islam. Mathematical modeling of microbial enhanced oil recovery. spe-20480. Technical report, presented at ATCE, New Orleans, Louisiana, USA, 23–26 September, 1990.

E. Lacerda, C. Da Silva, V. I. Priimenko, A. P. Pires, et al. Microbial eor: a quantitative prediction of recovery factor. In *SPE Improved Oil Recovery Symposium*. Society of Petroleum Engineers, 2012.

L. W. Lake. *Enhanced oil recovery*. Prentice Hall Englewood Cliffs, 1989.

D. Landa Marban. Modeling and simulation of microbial enhanced oil recovery: A new approach which includes the role of interfacial area. Master's thesis, The University of Bergen, 2016.

L. D. Landau and E. M. Lifchitz. *Physique théorique. Tome VI, Mécanique des fluides*. Editions Mir, 1971.

I. Lazar, I. Petrisor, and T. Yen. Microbial enhanced oil recovery (MEOR). *Petroleum Science and Technology*, 25(11):1353–1366, 2007.

R. J. LeVeque. *Finite volume methods for hyperbolic problems*, volume 31. Cambridge university press, 2002.

K.-A. Lie. An introduction to reservoir simulation using matlab: User guide for the matlab reservoir simulation toolbox (MRST). *SINTEF ICT, May*, 2014.

J. Lobry. Le modele de michaelis-menten, 2008.

R. I. Masel. *Principles of adsorption and reaction on solid surfaces*, volume 3. John Wiley & Sons, 1996.

S. M. Nielsen, A. Shapiro, E. H. Stenby, and M. L. Michelsen. Microbial enhanced oil recovery-advanced reservoir simulation. *Department of Chemical and Biochemical Engineering*, 2010a.

S. M. Nielsen, A. A. Shapiro, M. L. Michelsen, and E. H. Stenby. 1d simulations for microbial enhanced oil recovery with metabolite partitioning. *Transport in porous media*, 85(3):785–802, 2010b.

J. M. Nordbotten and M. A. Celia. *Geological storage of CO2: modeling approaches for large-scale simulation*. John Wiley & Sons, 2011.

L. Romero-Zerón. Introduction to enhanced oil recovery (EOR) processes and bioremediation of oil-contaminated sites. *Croatia: InTech*, 2012.

P. Shen, B. Zhu, X.-B. Li, Y.-S. Wu, et al. The influence of interfacial tension on water-oil two-phase relative permeability. In *SPE/DOE Symposium on Improved Oil Recovery*. Society of Petroleum Engineers, 2006.

K. Skiftestad. Numerical modelling of microbial enhanced oil recovery with focus on dynamic effects: An iterative approach. Master's thesis, Universitetet i Bergen (UiB), 2015.

M. Thullner. Comparison of bioclogging effects in saturated porous media within one-and two-dimensional flow systems. *Ecological Engineering*, 36(2):176–196, 2010.

M. Todd, W. Longstaff, et al. The development, testing, and application of a numerical simulator for predicting miscible flood performance. *Journal of Petroleum Technology*, 24(07):874–882, 1972.

B. Volesky. Sorption and biosorption. bv sorbex, inc. quebec: Mcgill university, 2003. 316 p. Technical report, ISBN 0-9732983-0, 2003.

Wikipedia. Extraction-of-petroleum. Wikipedia, the Free Encyclopedia, https://en.Wikipedia.org/wiki/Extraction-of-petroleum/, Accessed February 27, 2017 (21:34)a.

Wikipedia. Michaelis-meneten-kinetics. Wikipedia, the Free Encyclopedia, https://en.wikipedia.org/wiki/Michaelis-Meneten-Kinetics., Accessed March, 18 2017 (11:05)b.

T. F. Yen. *Microbial enhanced oil recovery*. CRC press, 1989.